

MSEC_ICM&P2008-72547

A GENERIC TOOL PATH GENERATION METHODOLOGY FOR INCREMENTAL FORMING

Rajiv Malhotra

Department of Mechanical Engineering, Indian Institute of Technology Kanpur, Kanpur, India.

N Venkata Reddy

Department of Mechanical Engineering, Indian Institute of Technology Kanpur, Kanpur, India. nvr@iitk.ac.in

Jian Cao

Department of Mechanical Engineering, Northwestern University,
Evanston, IL, 60208
jcao@northwestern.edu

ABSTRACT

This paper presents a generic methodology for tool path generation for an arbitrary component that can be formed by single point incremental forming (SPIF) to obtain required geometrical accuracy. Adaptive slicing concepts used in layered manufacturing have been modified and used for generating tool path for SPIF. Experiments and FEA have been carried out to study the effectiveness of the proposed methodology. Results indicate that the proposed methodology enhances the accuracy achievable in SPIF.

KEY WORDS: SPIF, automatic generation of contour and helical tool paths, accuracy and surface finish,

INTRODUCTION

Conventional sheet metal forming operations require component specific and costly tooling and their design and fabrication add to the lead-time. Incremental forming is one of the technologies that have emerged as an alternative to conventional sheet metal forming processes for mass customization. However, before this process can be used in industrial applications, the ability to automatically generate a tool path based on the required final shape of the sheet has to be developed.

In single point incremental forming (SPIF), tool path significantly influences the forming limits, accuracy, surface quality, thickness variation as well as forming time. There have been reasonable number of attempts to study various tool paths and their effect on the above mentioned aspects. Almost all these attempts are either component specific or are based on trial-and-error approach. Most of them have used the contour tool path generated using the surface milling module of commercial CAM software. It has been observed that the deformation at the starting and end points of each contour is biaxial, and along the path is plane strain stretching [1]. In biaxial stretching, the equivalent strain is always higher than that in

plane strain stretching, which leads to failure at the biaxial point. In addition, contour tool path strategy leaves marks at the end points. To avoid the accumulation of strains due to biaxial stretching and the tool marks at the end points, Filice et al. [2] suggested using a 3D helical tool path. A helical tool path is a continuous 3D curve with incremental descent of the tool distributed over the complete contour of the part.

Kim and Yang [3] generated tool paths for symmetric parts, such as a clover cup and an ellipsoidal cup, using closed form equations. Kopac and Kampus [4] examined various forming procedures for forming symmetric components, in terms of tool movement: a) from exterior to interior, b) from interior to exterior, c) first in the center then from exterior to interior and d) first in the center then from interior to exterior, and reported that the maximum depth of forming can be achieved with case (d). Bambach et al. [5] studied two tool path strategies: contour and radial for in-plane movement (center to outer) coupled with two z-movement strategies: conventional and conical, for producing only conical parts. It was concluded that the conventional/contour strategy is better than radial strategies. Recently, Skjoedt et al. [6] generated helical paths for asymmetric components using a combination of the surface milling module of PRO-E to produce contour paths and their own code to produce helical paths from these contour paths. Even though this approach successfully demonstrates the tool path generation capabilities offered by commercial software, the requirements of tool path generation in SPIF may not be represented adequately. Verbert et al. [7] developed an iterative method for tool path generation but used STL files which have chordal errors as an inherent drawback and have only generated contour tool paths.

The objective of the present work is to automate the process of tool path generation to form an accurate sheet metal component using SPIF. To achieve the same, slicing strategies similar to those used in layered manufacturing (LM) [8] are

adapted in this work. Subsequently the helical tool path is generated from these contour paths. Compensation for both tool shape and tool size has been implemented for contour and helical tool paths.

TOOL PATH GENERATION

Adaptive slicing methodologies [8] are used in Layered manufacturing to ensure the geometrical accuracy and improve surface finish of the parts produced by layer wise material deposition. A similar concept has been used to generate contour tool paths by finding intersections of a shell based model of the component with infinite planes at decreasing z-heights starting from the top of the model. Slicing is carried out from the top of the part because in SPIF the tool usually starts forming the blank into the desired component from the top of the component. Methodology developed for tool path generation is illustrated in detail using the CAD model of the part shown in Fig.1, as an example.

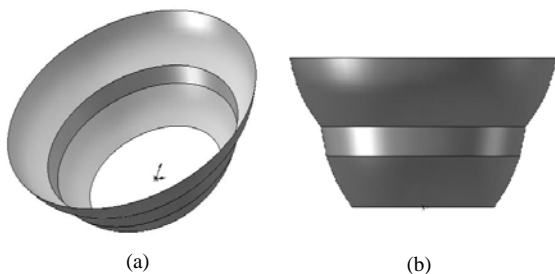


Figure 1. CAD model of the component used to illustrate adaptive slicing (a) Isometric view (b) Profile view

Given component is divided into zones in the z direction based on transitions in the type of surface characterizing the part geometry, as shown in Fig.2. Subsequently, slices are generated in each zone using the maximum slice thickness specified by the user. The slice heights thus generated in all the zones are stored sequentially in an array *initial_hts*.

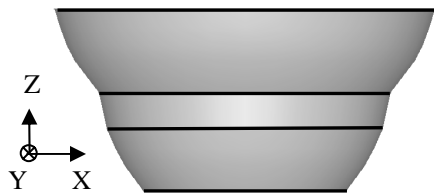


Figure 2. Slices at the zonal junctions

In order to use a volumetric error based adaptive slicing criterion, the region between two consecutive slices and the ruled solid formed by lofting one slice onto another are obtained. Consider as an example the slices shown in Fig. 3.

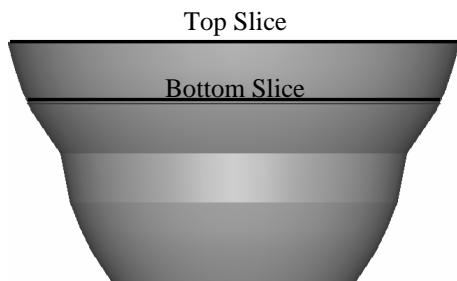


Figure 3. Two slices generated on the CAD model

The bottom slice is lofted onto the top slice to generate a ruled surface. The planar surfaces bounded by the top and bottom slices are sewn together with this ruled surface to make a closed shell. This closed shell is used to make a solid, whose volume is stored as *lofted_volume*. The part of the shell model above the top slice and that below the bottom slice were cut off using the Boolean cut operation and the resultant shell i.e. *cut_shell* is obtained. The planar surfaces bounded by the top and bottom slices are sewn together with *cut_shell* to make a closed shell. This closed shell is used to make a solid and the volume of this solid is stored as *part_volume*. The volumetric error i.e. *vol_error* for the region between these two slices is now calculated using Eqn. (1).

$$vol_error = \frac{|(part_volume - lofted_volume)|}{part_volume} \times 100 \quad (1)$$

At the same time the areas of the plane surfaces bounded by the top and bottom slices are obtained as *area_top* and *area_bottom* respectively. The *area_error* is calculated between the two slices using Eqn (2).

$$area_error = \frac{|area_top - area_bottom|}{area_bottom} \times 100 \quad (2)$$

Volumetric error and area error are used as heuristic measures of geometrical accuracy and surface finish, respectively. If *vol_error* between these two slices is above the user specified limit (*vol_error_max*) or if *area_error* is greater than the user specified limit (*area_error_max*), then a slice is inserted halfway between these two slices, provided that the distance between the bottom slice and the newly inserted slice does not go below the user specified minimum slice thickness (*h_min*). Then, the steps from Step 2 onwards are repeated for the lower slice and the newly inserted slice, and if required another slice is inserted in between these two. At the same time the array *initial_hts* is updated so that these new slices are included in the right order. Once there is no further need for slice insertion Step 3 is repeated for the next pair of consecutive slices, and so on till the entire array *initial_hts* has been processed. The above procedure is illustrated in Fig.4.

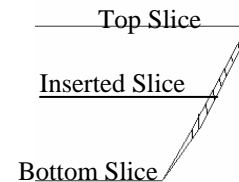


Figure 4. Schematic showing slice insertion

The final output after adaptive slicing is a modified array *initial_hts* which contains the slice heights satisfying the user specified constraints on geometrical accuracy and surface finish. This modified array will henceforth be referred to as *final_hts*. Contour paths are generated by computing intersections of the part with an infinite plane at the z-height values stored in *final_hts* and a fixed number of points N are generated on each contour. The contour paths generated with

and without adaptive slicing are shown in Figs. 5(a) and 5(b), respectively.

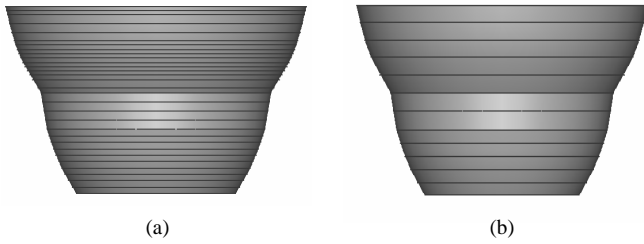


Figure 5. Slices generated (a) using adaptive slicing (b) without using adaptive slicing

After adaptive slicing, it is assumed that the surface between the two slices is a ruled surface. The helical path is generated from contour tool paths generated after adaptive slicing. Starting from the top slice, the j^{th} point of the $(i-1)^{\text{th}}$ helical path segment is generated using Eqn. (3)

$$x_j = s_j p_j + (1 - s_j) p_j^0 \quad (3)$$

where,

$$s_j = \frac{\sum_{l=j-1}^{l=N-1} |p_{l+1} - p_l|}{\sum_{l=1}^{l=N-1} |p_{l+1} - p_l|}$$

p_l is the l^{th} point on the i^{th} slice and p_l^0 is the l^{th} point on the $(i-1)^{\text{th}}$ slice. These generated points are stored in an array *helical_points*. Figures. 6(a) and 6(b) show the helical tool path generated with and without adaptive slicing respectively.

In this work a hemispherical ended tool of radius R attached to a 3-axis CNC milling machine is considered as the forming tool. The points generated earlier on contour/helical tool paths are contact points at which the hemispherical end of the tool should be tangential to the intended part surface. Since the tip of the tool is used as the reference point on CNC machines, compensation for the tool radius R is provided as illustrated in Fig. 7. First, the normal to the part surface ' n ' at a contact point is computed. The centre of the hemispherical end (T_{ce}) is computed using Eqn. (4).

$$T_{ce} = T_{cp} + R \cdot \hat{n} \quad (4)$$

The coordinates of the tool tip T_{tip} are obtained using Eqn. (5).

$$T_{tip} = T_{ce} - (0 \hat{i} + 0 \hat{j} + R \cdot \hat{k}) \quad (5)$$

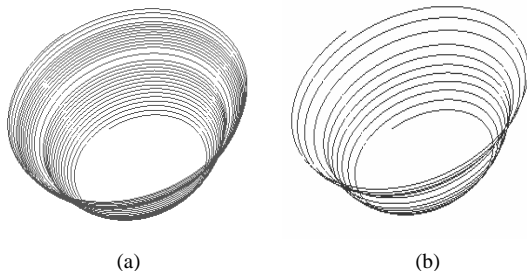


Figure 6. Helical path generated (a) with adaptive slicing (b) without adaptive slicing

The above procedure is repeated for all the contact points and the tool tip coordinates for the entire tool path are generated.

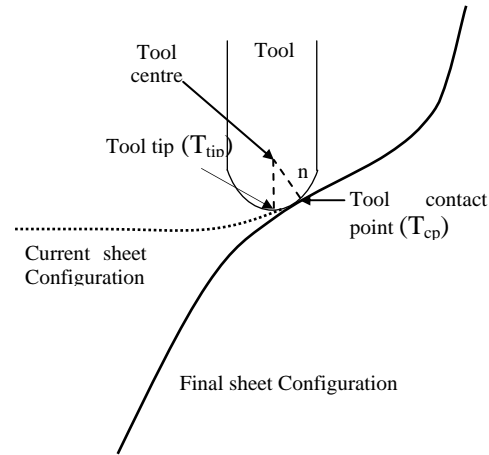


Figure 7. Schematic showing methodology for tool radius compensation

In the absence of tool radius compensation, the hemispherical tool would gouge into material that should not be deformed and this will adversely affect part accuracy. Figure 8 shows how tool radius compensation prevents gouging by the tool.

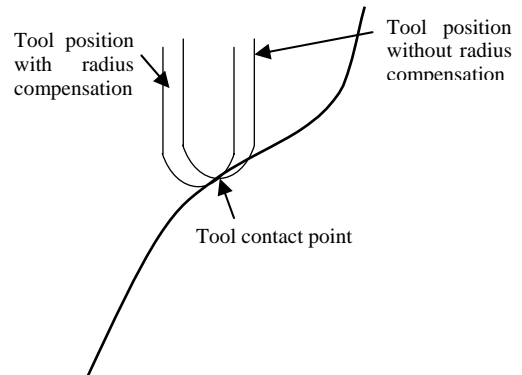
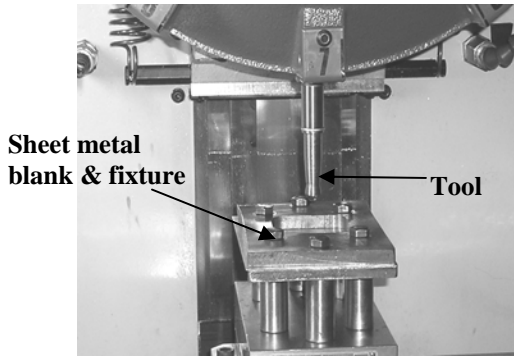


Figure 8: Schematic showing gouging in absence of tool compensation

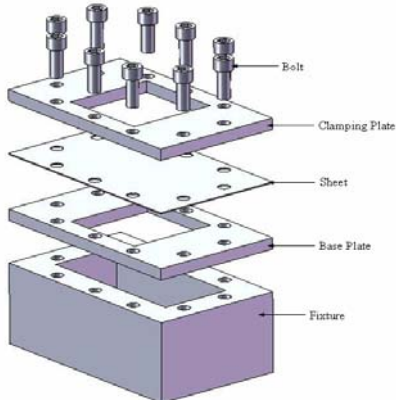
RESULTS AND DISCUSSION

The methodology presented above is implemented using OpenCascade (version 6.1) libraries in a VC++ programming environment. The geometry of the component to be formed is taken as input in a neutral file format (STEP) along with the user defined parameters mentioned earlier. The program is executed on a desktop PC using an Intel® Pentium® 4 3.06 GHz processor with 2GB of RAM. In this section two case studies (an axi-symmetric cone and an asymmetric freeform component) are considered to demonstrate the tool path generation methodology presented above.

The experimental setup used for SPIF during the present work is shown in Fig. 9. The tool has a hemispherical forming end of diameter 6.5 mm. The blank material is aluminum (AL 5052) and machine oil is used to lubricate the tool-blank interface.

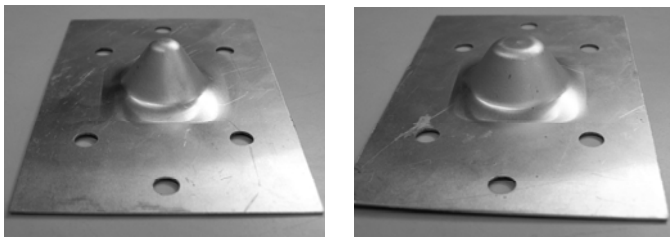
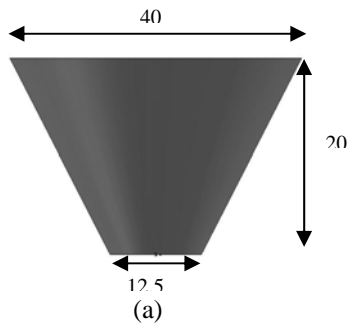


(a)



(b)

Figure 9. (a) EMCO 3-axis milling machine used as the CNC platform. (b) Schematic of clamping fixture used



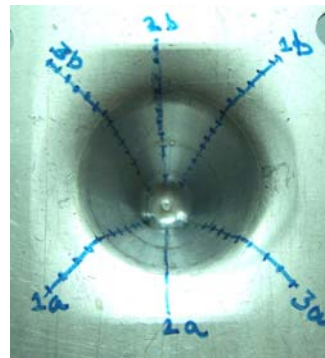
(b)

(c)

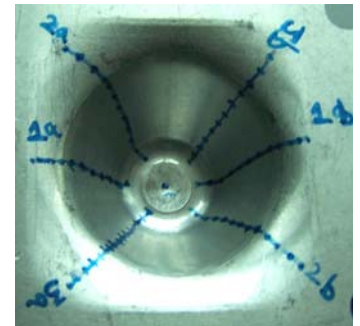
Figure 10 (a) CAD model of cone to be formed (b) Cone formed using helical toolpath with tool compensation (c) Cone formed without helical toolpath with tool compensation

Axi-symmetric cone:

Helical tool paths with and without tool compensation are generated for a conical component shown in Fig. 10(a) and are used to form the components shown in Figs. 10(b) and 10(c), respectively. Deformed geometry of the components is measured along the symmetric axes shown in Fig. 11, using a CMM. Figures 12 and 13 clearly show that the use of tool compensation leads to better geometrical accuracy of the formed component. To observe the effect of bending more clearly, an octagonal component is formed (Fig. 14(a)). The geometric deviation of the topmost contour of the octagon is measured along the lines shown in Fig. 14(b), using a CMM. The deviation of formed geometry is more when the uppermost contour is further away from the fixture opening (Fig 14(c)).

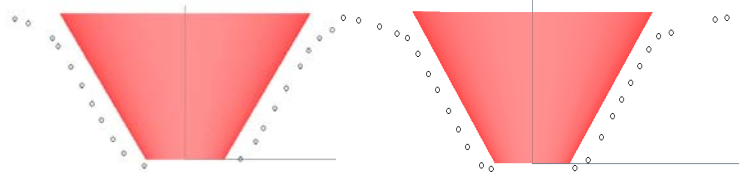


(a)



(b)

Figure 11. Sections along which the profile is measured for the cone formed (a) with tool shape compensation (b) without tool shape compensation



(a)

(b)

Figure 12. Measured profile (points) and desired profile (CAD model) for the cone formed without using tool compensation (a) along section 1a-1b (b) along section 2a-2b



(a)

(b)

Figure 13. Measured profile (points) and desired profile (CAD model) for the cone formed with tool compensation (a) along section 1a-1b (b) along section 2a-2b

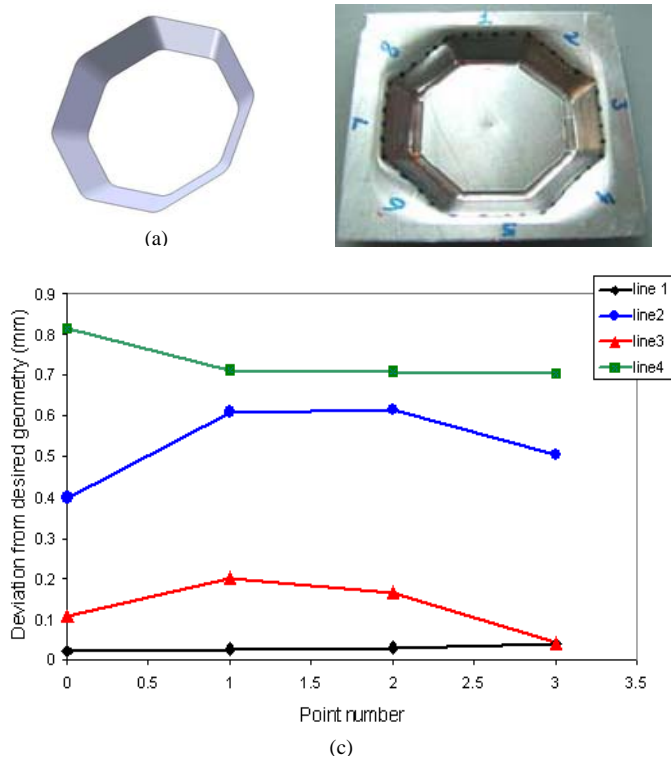


Figure 14. (a) CAD model of octagonal component (b) Points along which the profile of the top contour is measured (c) Error graph

Finite element analysis of SPIF is carried out using the ABAQUS 6.5 package. The sheet metal blank is modeled as a plane deformable sheet made up of 4-noded quadrilateral shell elements with reduced integration. The tool is modeled as an analytical rigid body of the same geometry as that used in experiments. The tool-blank interface is considered to be frictionless. Comparison of the formed shapes predicted by FEA for helical tool paths (with and without tool compensation) and CAD model of the desired component shows that the component formed using tool radius compensation (Fig. 15(a)) is closer to the desired shape of the component. However, it can also be seen that after compensating for tool radius there is a significant geometrical error near to the top of the component. As discussed earlier, this can be attributed to bending.

Asymmetric freeform shape:

Contour and helical tool paths are generated for the component shown in Fig. 16. The primary aim of fabricating this component is to demonstrate the capability of the tool path generation methodology to generate tool paths for freeform non-symmetric shapes. The tool paths shown in Fig. 17(c) and 17(d) are used to fabricate the desired component and the formed components are shown in Fig. 18(a) and 18(b), respectively. It can be clearly seen that the use of adaptive slicing enhances the conformity between the formed and the desired components.

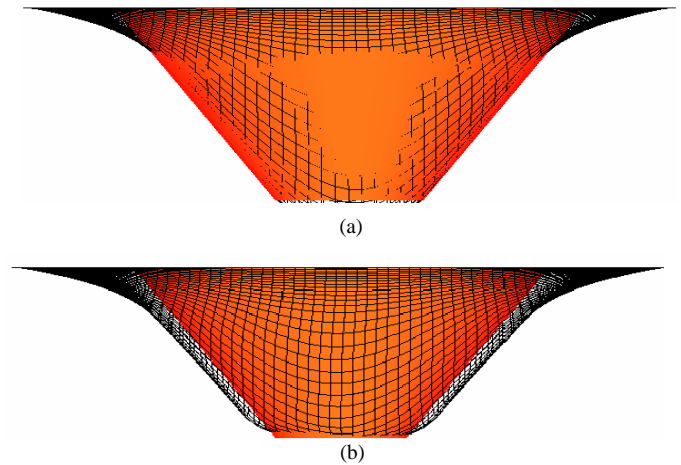


Figure 15. Comparison of shape predicted by FEA and desired shape when (a) tool radius compensation is used (b) tool radius compensation is not used

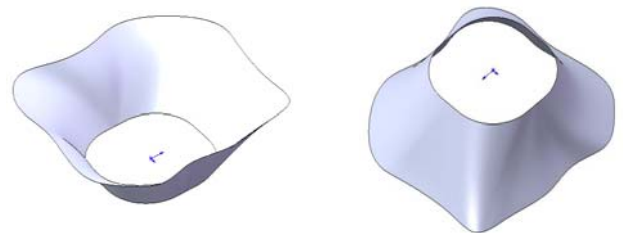


Figure 16. CAD model of the freeform component

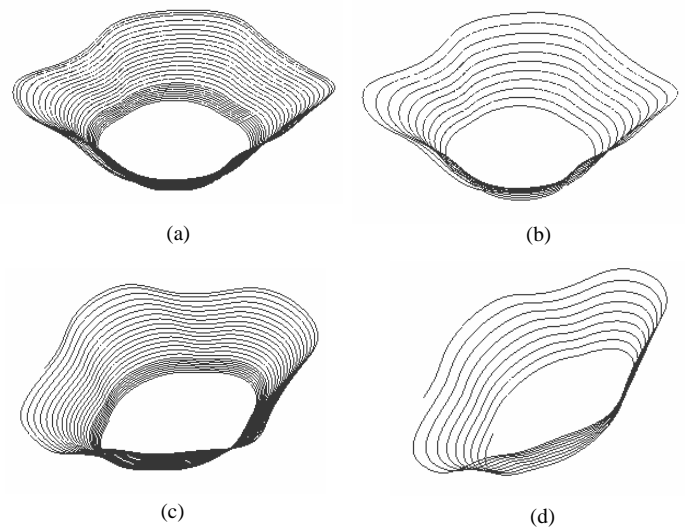
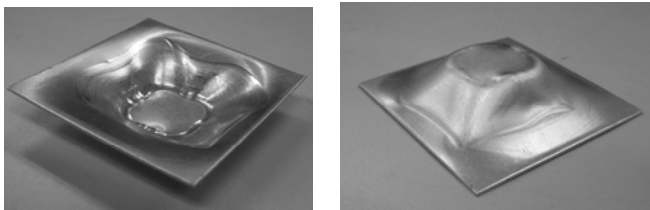
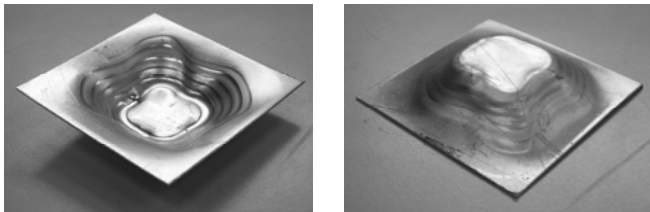


Figure 17. (a) Contour tool path with adaptive slicing (b) Contour tool path without adaptive slicing (c) Helical tool path with adaptive slicing (d) Helical tool path without adaptive



(a)



(b)

Figure 18. Component formed using helical tool path
(a) with adaptive slicing (b) without adaptive slicing

CONCLUSIONS

The aim of this work was to develop and implement a platform-independent generalized methodology for the generation of contour and helical tool paths, for an arbitrary component formable by SPIF. The constraints on the tool path are that the formed component should have required geometrical accuracy and surface finish. Adaptive slicing techniques used in layered manufacturing have been modified and used for this purpose. The developed methodology has been shown to be usable for axi-symmetric as well as asymmetric components that can be formed by SPIF within the same setup. The tool paths generated have been used to form components whose geometry conforms closely to the geometry of the desired component. It has been shown that bending is the major factor causing geometrical inaccuracies in the formed component.

ACKNOWLEDGMENTS

Authors would like to acknowledge Department of Science and Technology, New Delhi and NSF of USA for the financial support to carry out the present work. Authors also acknowledge Indo-US Science and Technology Forum for providing the travel support to carry out this collaborative work.

REFERENCES

- [1] Jeswiet, J., 2005, Asymmetric incremental sheet forming, *Advanced Materials Research*, Vol. 6-8, 35-58.
- [2] Filice, L., Fratini, L., and Micari, F., 2002, Analysis of Material Formability in Incremental Forming, *Annals of the CIRP*, V 51 (1), 199-202.
- [3] Kim, T. J. and Yang, D. Y., 2000, Improvement of formability for the incremental sheet metal forming process,

International Journal of mechanical Sciences, Vol. 42, 1271-1286.

[4] Kopac, J. and Kampus, Z., 2005, Incremental sheet metal forming on CNC Milling Machine-Tool, *Journal of Materials Processing Technology*, Vol. 162-163, 622-628.

[5] Bambach, M., Ames, J., Azaouzi, M., Campagne, L., Hirt, G., and Batoz, J.L., 2005, Initial Experimental and Numerical Investigation into a Class of New Strategies for Single Point Incremental Sheet Forming (SPIF) *Rapid prototyping and Rapid Tooling* ESA FORM 2005 Conference, 671-674.

[6] Skoejdt M. et.al, 2007, Creating Helical Tool Paths for Single Point Incremental Forming, *Key Engineering Materials*, Vol. 344, 583-590

[7] Verbert et.al, 2007, Feature based approach for increasing the accuracy of the SPIF process, *Key Engineering Materials*, Vol. 344(2007), 527-534

[8] Pandey P.M et.al, 2003, Slicing procedures in layered manufacturing, *Rapid Prototyping Journal*, Volume 9, number 5, 274-288.